Received: 3 November 2020 | Revised: 6 January 2021 | Accepted: 9 January 2021

DOI: 10.1002/jcp.30291

RESEARCH ARTICLE

Journal of Cellular Physiology WILEY

Mesenchymal stem cell-derived extracellular vesicles conditionally ameliorate bone marrow failure symptoms in an immune-mediated aplastic anemia mouse model

Mohammad A. Gholampour[1] | Saeid Abroun PhD[1] | Rienk Nieuwland[2,3] | Seyed J. Mowla[4] | Sara Soudi[5]

[1]Department of Hematology, Faculty of Medical Sciences, Tarbiat Modares University, Tehran, Iran

[2]Laboratory of Experimental Clinical Chemistry, Amsterdam UMC, Location AMC, University of Amsterdam, Amsterdam, The Netherlands

[3]Vesicle Observation Centre, Amsterdam UMC, Location AMC, University of Amsterdam, Amsterdam, The Netherlands

[4]Department of Molecular Genetics, Faculty of Biological Sciences, Tarbiat Modares University, Tehran, Iran

[5]Department of Immunology, Faculty of Medical Sciences, Tarbiat Modares University, Tehran, Iran

Correspondence
Saeid Abroun, Department of Hematology, Faculty of Medical Sciences, Tarbiat Modares University, Tehran 14115-111, Iran.
Email: abroun@modares.ac.ir

Funding information
Iran National Science Foundation, Grant/Award Number: 98013002; Council for Development of Stem Cell Sciences and Technologies: 11/35732; Tarbiat Modares University, Grant/Award Number: 9620822001

Abstract

Acquired forms of Aplastic anemia (AA) are characterized by T cell-mediated immune disease resulting in bone marrow (BM) failure and marrow hypoplasia. In these cases, it is a major challenge to modulate autoreactive T cell activity and thereby decrease the pro-inflammatory cytokine storm. Emerging evidence indicates that extracellular vesicles derived from mesenchymal stem cells (MSC-EVs) control and modulate immunity. The therapeutic potential of MSC-EVs has not been investigated in acquired AA. Hence, in this study, we constructed an AA mice model through irradiation and splenocyte infusion to test the benefits of hypoxic MSC-EVs (Hx-EVs) and normoxic MSC-EVs (Nx-EVs). We found that MSC-EVs treatment significantly prolonged the survival rate and increased the platelet (PLT) counts of the AA mice. Immunohistochemical staining and colony assay confirmed amelioration of hypoplasia in the BM and increased numbers of hematopoietic stem cells (HSCs). These effects of MSC-EVs were mediated by T cell suppression and inhibition of interferon-gamma (IFN-γ) and tumor necrosis factor-alpha (TNF-α) production in the AA mouse model. In addition, an in vitro study revealed that MSC-EVs led to reduced IFN-γ and TNF-α levels and there was an association with decreased splenocyte viability. Previous studies examined the diagnostic and prognostic values of microRNAs (miRNAs) in AA and identified miR-199a, miR-146a, miR-223, and miR-126. We used quantitative real-time PCR to evaluate the expression of these miRNAs on isolated BM mononuclear cells (BM-MNCs) from treated and untreated AA mice. miR-223, miR-146a, and miR-199a expressions increased in the MSC-EVs treated AA mice. Treatment with MSC-EVs increased expression of miR-223 and miR-146a. Our findings showed that treatment with MSC-EVs significantly ameliorated immune destruction of HSCs in the AA mouse model and confirmed the importance of miRNAs in the clinical status of this model.

KEYWORDS

aplastic anemia, extracellular vesicle, hematopoietic stem cells, mesenchymal stem cells, microRNA

1 | INTRODUCTION

Aplastic anemia (AA) is a type of rare bone marrow (BM) failure syndrome. Although AA may be acquired, it can also have other causes. In its severest form, AA is associated with a high mortality. AA is characterized by a reduction in the number of hematopoietic stem cells (HSCs), which causes pancytopenia, and a morphologically and functionally "empty" BM (Hosokawa et al., 2017). There are two types of AA—inherited and acquired. Hereditary AA occurs by gene defects and is usually diagnosed in childhood; Moreover, this form of AA is rare compared to the acquired. Most acquired cases are triggered by environmental exposure to toxins, drugs, radiation, and viral infections in addition to its potential idiopathic causes (Brzeźniakiewicz-Janus et al., 2020). Generally, the underlying pathophysiology for initiation and pathology of acquired AA is believed to be immune-mediated T cells that cause the destruction of HSCs. Therefore, the majority of AA patients respond to immunosuppressive therapies (ISTs), which provides the best proof for an underlying immune pathophysiology. Currently, the standard first-line immunosuppressive regimens are anti-thymocyte globulins (ATGs) and cyclosporine, which lead to hematological improvement by causing transient depletion of T cells (Giudice et al., 2018). Although activated T cells are considered to play a role in the pathology of immune-mediated AA, much less is known about the molecular basis of the underlying T cell activation (Boddu & Kadia, 2019).

Emerging evidence shows the immunomodulatory effect of mesenchymal stem cells (MSCs) in a myriad of inflammatory diseases. This immunoregulatory capacity suggests that MSCs could be promising candidates for cell therapy because of their capacity for governing inflammation and restraining immune cells (Fan et al., 2020; Weiss & Dahlke, 2019). Although the therapeutic potential of MSCs has been reported in various preclinical studies, several critical limitations exist with MSC therapy. Since MSCs are isolated from distinct individuals and act as "living material," a major hurdle is the quality control needed for the use of MSCs for therapeutic purposes (Weiss & Dahlke, 2019).

The therapeutic efficacy of MSCs could be affected by several factors such as the isolation protocol, culture conditions, storage procedure, and administration method. These factors affect cell viability and efficacy, and result in elevated costs and reproducibility. Additional genetic modifications could boost the therapeutic potency of MSCs; therefore, MSCs should be monitored and evaluated to prevent unexpected safety concerns like ectopic differentiation and tumor formation (Phelps et al., 2018). For these reasons, researchers have considered extracellular vesicles derived from MSCs (MSC-EVs) as promising candidates for cell-free therapy since EVs approximate the immunomodulatory characteristics of MSCs (Trubiani et al., 2019). Extracellular vesicles (EVs) are cell-derived nanoparticles released by all cell types. EVs play a role in intercellular communication by transporting biomolecules to maintain homeostasis and prevent disease. The positive effects of MSCs may remain for an extended duration following in vivo administration and after the disappearance of the MSCs. This may explain the long-lasting effects of MSC culture conditioned medium. Therefore, MSC-EVs may provide an important advantage over MSC-mediated immune suppression (Seo et al., 2019). It has been reported in multiple studies that the therapeutic effects of MSCs are mediated by EVs. Thus, MSC-EVs may, at least in part, exert protective paracrine effects. Evidence that cargo of MSC-EVs includes cytokines, metabolites, lipids, and microRNAs (miRNAs) supports the idea that MSC-EVs may have similar regenerative and anti-inflammatory effects (Eleuteri & Fierabracci, 2019).

Increasing numbers of studies have shown that hypoxia can regulate the release of exosomes and change their contents. It has been reported that that hypoxia can stimulate cells to release more EVs, and change the EVs cargoes, which include selective proteins and miRNAs (Duan et al., 2019). The quality and therapeutic function of MSCs-EVs is promoted by factors such as hypoxic preconditioning of BM-MSCs and stimulation with IFN-γ (Ren et al., 2019; Zhang et al., 2020). In some hypoxic studies, MSC-EVs derived from hypoxic conditions had a therapeutic and protective effect via multifunctional processes that involve negative regulation of the apoptotic process, downregulation of oxidative stress, promotion of angiogenesis, and antifibrotic mechanisms (Duan et al., 2019).

miRNAs are endogenous, short noncoding RNAs (21–25 nucleotides in length) that modulate posttranscriptional regulation of gene expression by promoting translational repression or degradation of their target mRNAs. miRNAs are involved in both physiological and pathological processes (Canzano et al., 2018). Aberrant expressions of immune-related miRNAs have been associated with immune-mediated diseases. In terms of previous studies, miR-199a, miR-223, and miR-146a in MSC-EVs have been shown to attenuate the immune responses in patients with sepsis, colitis, muscle injury, and hepatitis (Chen et al., 2018; Lo Sicco et al., 2017; Song et al., 2017; Wang et al., 2015; Wu et al., 2019; Zhang, 2016).

In the current study, we first examined the effects of hypoxic MSC-EVs (Hx-EVs) and normoxic MSC-EVs (Nx-EVs) on the expression levels of miR-199a, miR-146a, miR-223, and miR-126, and proliferation as well as pro-inflammatory cytokine production (TNF-α and IFN-γ) in vitro. We also established a mouse model of AA to examine the in vivo effects of Hx-EVs and Nx-EVs.

2 | MATERIALS AND METHODS

2.1 | Mice

C57BL/6 ($H^{b/b}$) and BALB/c ($H^{d/d}$) mice were purchased from the Pasteur Institute of Iran. Then, hybrid B6F1 ($H^{b/d}$) mice were generated by crossing the C57BL/6 mice with BALB/c mice. Age- and sex-matched controls were used. The mice were bred and maintained in cages in the Animal Laboratory of Tarbiat Modares University, Tehran, Iran, and received standard care and nutrition. The study protocols were approved by the Tarbiat Modares University Animal Care and Use Committee.

2.2 | Isolation of BM-MSCs and cell culture

The 3- to 4-week-old male inbred C57BL/6 mice were killed to isolate BM-MSCSs. Femurs and tibiae were dissected and cleared of connective tissue. BM was flushed with 2 ml Dulbecco's modified Eagle's medium

(DMEM, Gibco, Invitrogen Corporation) supplemented with 15% fetal bovine serum (FBS, Gibco, Invitrogen Corporation) and 1% penicillin/streptomycin (Gibco, Invitrogen Corporation, Grand Island, NY). The cells were seeded in 60 mm^2 tissue culture plates (SPL Life Sciences) at a density of 4×10^6 cells and incubated for 3 h in a humidified incubator at 37°C with 5% CO_2. After 3 h, nonadherent cells were removed by changing the medium. Thereafter, the medium was changed every 3 days. The cells were detached when they reached 80% confluency by using 0.25% Trypsin-EDTA (Gibco, Invitrogen Corporation) and seeded in 75 cm^2 flasks (SPL Life Sciences). The medium was refreshed every 3 days. Once the cells reached 80%–85% confluency, the medium was replaced by an EV-depleted medium. A prior elimination of EVs from FBS is crucial. The EVs were depleted from FBS by an ultrafiltration-based protocol (Kornilov et al., 2018). The cells were incubated under hypoxic (5% O_2) and normoxic (21% O_2) conditions. Then, the conditioned medium was collected every 2 days. The collected medium was centrifuged for 10 min at 300*g* to remove viable cells, and the supernatant was centrifuged for 15 min at 5000*g* to remove debris. The EV-containing supernatant was stored at −80°C until use.

In vitro experiments were performed to assess the effect of MSC-EVs on splenocytes. Analyses were performed using the freshly isolated C57BL/6 mouse spleens. The spleens were collected and placed in ice-cold phosphate-buffered saline (PBS, Gibco, Invitrogen Corporation). The spleens were homogenized by pushing through a 70 μm cell strainer with a syringe plunger to remove tissue debris. The red blood cells (RBCs) were lysed by ammonium chloride. And then, the splenocytes were grown in an EV-depleted medium that contained RPMI-1640 supplemented with 15% EV-depleted FBS. For T cell activation, isolated splenocytes were cultivated in a conventional medium containing 120 pg/ml phorbol 12-myristate 13-acetate (PMA; Sigma Chemical Co.) and 120 IU/ml interleukin-2 (IL-2; BD Pharmingen, Inc.). After 48 h, the cells were seeded in six-well culture plates and treated with 50 μg EVs derived from hypoxic (Hx-EVs) and normoxic (Nx-EVs) MSC conditioned medium for 24 and 48 h. Finally, the cells were harvested for downstream analysis.

2.3 | Identification of BM-MSCs

The purity of isolated BM-MSCs was determined by flow cytometry. Passage-2 adherent cells were detached and suspended to generate 1×10^6 cells/ml. The suspension was washed with PBS and resuspended. The purity of the BM-MSCs was analyzed using antibodies against CD73, CD90, CD105, CD34, CD45, and HLA-DR (R&D Systems) with a FACSCalibur (Becton Dickinson).

For in vitro osteogenic induction, BM-MSCs were seeded and grown until 70% confluency and then cultured in osteoinductive α-minimal essential medium (α-MEM) that contained 50 mg/mL L-ascorbic acid-2-phosphate, 10 mM glycerol 2-phosphate disodium salt, 0.1 nM dexamethasone, and 200 ng/ml recombinant bone morphogenic protein-2 (rBMP-2) for 3 weeks. For adipogenic induction, the cells were cultured with α-MEM that contained 10% FBS, 10 ng/ml insulin, and 1×10^{-8} M dexamethasone for 3 weeks. The medium was changed every 3 days for both adipogenic and osteogenic induction. The osteogenic and adipogenic differentiation was determined by alizarin red S and oil red O staining, respectively.

2.4 | Extracellular vesicle isolation

First, 100 ml of collected conditioned medium was loaded onto Amicon Ultra-15 Centrifugal Filter Units (MWCO: 100 kDa; Merck Millipore). Next, conditioned media was concentrated to ≤1 ml by repeated centrifugation at 4000*g*. The filter membrane was washed with 500 μl PBS and centrifuged at the same speed according to the previous step. Then, the concentrate was collected and processed by size exclusion chromatography (SEC) as described by Böing et al. (2014) with some adaptations. In brief, 1 ml of concentrated media was applied to a 10 ml Sepharose CL-2B column (GE Healthcare Life Sciences) and 24 fractions of 0.5 ml were collected using PBS as an eluent. The protein content of the fractions was determined using the BCA assay according to the manufacturer's instructions. The EV-containing fractions 8–10 were pooled and concentrated to 250 μl on an Amicon Ultra-4 Centrifugal Filter Unit (MWCO: 100 kDa; Merck Millipore) by centrifugation at 4000*g* and stored at −80°C.

2.5 | Immunoblotting

To confirm the presence of EVs, we determined the levels of CD9 and CD63. Briefly, BM-MSCs protein lysates were extracted using RIPA buffer supplemented with a cocktail of protease inhibitors (Thermo Fisher Scientific). The protein concentration of the lysate was determined using the BCA assay. Next, 20 μg of each BM-MSC cell lysate and EVs were loaded onto 12% (v/v) sodium dodecyl sulfate-polyacrylamide gel electrophoresis (SDS-PAGE). After electrophoresis, the proteins were transferred to a Polyvinylidene fluoride (PVDF) membrane (Roche). Then, nonspecific binding sites were blocked using 5% skimmed milk and washed with TBST that consisted of tris-buffered saline with 0.05% Tween-20. Next, the blots were stained with a primary anti-mouse CD9 (Sino Biological Inc.) and anti-mouse CD63 (BD Biosciences) diluted in TBST (1:1000) and incubated overnight at 4°C. The membranes were washed 3× with TBST and incubated with goat and rabbit HRP-conjugated secondary antibody for 1 h. The protein expression level was detected by the ECL Western blot analysis substrate (ECL, Amersham).

2.6 | Transmission electron microscopy

A total of 20 μL of the fresh MSC-EVs sample was pipetted onto a 300 mesh copper grid with a carbon film (AGS160-3) and incubated for 2 min. Then, excess liquid was removed by blotting. The resultant grid was rinsed twice with 20 μL of distilled water. After the washing step, 20 μL of 1% uranyl acetate was pipetted onto the grid and then incubated for

1 min. Finally, the grids were placed in a clean petri dish and transferred for transmission electron microscopy (TEM) imaging. The images were acquired using a Philips EM 208S transmission electron microscope at 80 kV.

2.7 | Determination of particle size by dynamic light scattering

The size distribution of the BM-MSC-derived EVs was determined using dynamic light scattering (DLS) by a Nanotrac Wave II (Microtrac, Inc.). Briefly, the volume of each MSC-EVs sample was increased up to 1 ml by PBS and loaded into a quartz cuvette, and measured at 25°C. Finally, the results were analyzed using FLEX software.

2.8 | Fluorescent labeling and internalization of extracellular vesicles

Fluorescent labeling of the purified EVs was performed using a PKH26 Fluorescent Cell Linker Kit (Sigma-Aldrich) according to the manufacturer's protocol. Splenocytes were seeded on 12-mm round coverslips (cell-culture grade, SPL Life Sciences) in 24-well tissue culture plates, and fluorescently labeled EVs were added to their culture media. For confocal microscopy imaging, target cells were incubated with labeled EVs for 6 h. Then, the cells were fixed with 10% formaldehyde (Mojallali), and the nuclei of the cells were stained with 4′,6-diamidino-2-phenylindole (DAPI; Sigma-Aldrich). The uptake of EVs was imaged using a spectral confocal microscope (Leica TCS SPE).

2.9 | Cell proliferation

Cell proliferation was determined using Cell Counting Kit-8 (Dojindo Molecular Technologies) following the manufacturer's specifications. Splenocytes were seeded onto a 96-well plate with 5×10^3 cells/well. Plates were incubated for 24 and 48 h at 37°C with 5% CO_2 in a humidified incubator. A total of CCK-8 reagent (10 μl) was added to each well and incubated at 37°C for 3 h. Absorbance readings were then taken at 450 nm using a microplate spectrophotometer (Anthos Biotech).

2.10 | Induction of the aplastic anemia model

The AA mouse model was developed from 8-week-old and sex-matched B6F1 mice. In our study, we also studied a serial dosage of irradiation, and 3Gy was finally selected because the complete blood count (CBC) and BM cellularity were not significantly different from those of the healthy control mice. First, the mice received sublethal irradiation (3Gy) with a 137 Cs source. After 4 h, AA was induced in the mice via an intraperitoneal (IP) injection of 5×10^7 splenocytes from C57BL/6 donors (Roderick et al., 2013). The AA mouse models received twice per week injections of 50 μg EVs as long as they were alive. The control group consisted of healthy untreated mice. The PBS group consisted of mice with AA that received intravenous (IV) administration of PBS. For the survival studies, we examined the mice twice a day. Mice were euthanized when there was a 20% loss of their initial body weight or if they were observed to be moribund. The mice were euthanized by CO_2 inhalation on the indicated day after induction of AA. The experiments were carried according to the protocols approved by Tarbiat Modares University (authorization reference number: 9620822001). All methods were performed in accordance with the relevant guidelines and regulations.

2.11 | Pathological observation

Femur bone tissue from AA and control mice was fixed in 10% formalin (v/v) overnight at room temperature. Subsequently, the specimens were decalcified at room temperature and embedded in paraffin. Next, the tissues were cut into sections that had a thickness of 3 μm, which were further deparaffinized and dehydrated using xylene and ethanol, respectively. Finally, the sections were stained with hematoxylin-eosin (H&E) and observed under an Olympus BX51 microscope (Olympus Corporation).

2.12 | Immunohistochemical analysis

The slides were deparaffinized and rehydrated. The endogenous peroxidase activity was blocked with 10% hydrogen peroxide for 10 min and the slides were washed with water. An antigen-retrieval procedure was performed by placing the slides in citrate buffer (10 mM citric acid, 0.05% Tween 20, pH = 6.0) inside a microwave oven for 10 min at 95°C. The slides were maintained in citrate buffer for 20 min until they became 25°C. All sections were washed two times with PBS and incubated with the Ki-67 antibody (Biocare Medical) at a 1:100 concentration at room temperature. The sections were washed twice and incubated with a secondary goat anti-rabbit IgG-HRP antibody (Kalazist, Iran) for 40 min. The signals were visualized with a DAB Chromogen Kit (Biocare Medical). The slides were counterstained with Mayer's hematoxylin, dehydrated, and mounted. We used ImageJ software (version 1.53e version, National Institute of Health Image program) for analysis.

2.13 | Complete blood count

Routine blood tests that included white blood cell (WBC), RBC, hemoglobin (Hb), and platelet (PLT) counts were evaluated with the blood taken from the heart of the mice. Blood indices were determined by an automatic hematology analyzer (Sysmex XT2000i

Hematology Analyzer; Sysmex Corporation). The experiments were performed in accordance with the manufacturers' protocols.

2.14 | Enzyme-linked immunosorbent assay

After collection of the cardiac blood, it was incubated for 20 min at room temperature, Then, cardiac blood was centrifuged at 1500*g* for 10 min at room temperature to collect the serum. Next, we determined the serum concentrations of tumor necrosis factor-alpha (TNF-α) and IFN-γ by enzyme-linked immunosorbent assay (BD Biosciences). Absorbance at 450 nm was measured using an Anthos 2020 microplate reader (Anthos Biotech).

2.15 | Colony assay

BM samples from EV-treated AA and control mice were harvested and subsequently treated with ammonium chloride to lyse RBCs. Next, mononuclear cells (MNCs) were isolated from the supernatant by density gradient centrifugation on Ficoll Hypaque (Lymphodex). A total of 4×10^4 cells were suspended in IMDM and cultured in murine semi-solid media (Methocult; Stemcell Technologies). The cells were maintained for 14 days at 37°C in a humidified atmosphere and 5% CO_2. The number of colonies was counted on Day 14.

2.16 | Quantitative real-time PCR

Total cellular RNA including miRNAs was extracted from 2×10^5 cells using TRIzol reagent (Thermo Fisher Scientific) following the manufacturer's instructions. The concentration and purity of the RNA samples were assessed as 260/280 nm and 260/230 nm ratios, respectively, using BioPhotometer 6131 (Eppendorf). cDNA was synthesized with a PrimeScript™ real-time PCR (RT-PCR) Kit according to the manufacturer's instructions (Takara Bio Inc.). cDNA synthesis for evaluation of miR-199, miR-126, miR-146a, and miR-223 was performed using Pars Genome miRNA Assay Kit according to the manufacturer's protocol (Pars Genome). Quantitative real-time PCR was performed using the StepOne Real-Time PCR System (Applied Biosystems). RNU6 was the internal control in the miRNA quantification.

3 | STATISTICAL ANALYSIS

The Kolmogorov–Smirnov test was used to calculate the normality of the sample distributions. Because the samples were normally distributed, one- and two-way ANOVA was used to assess the difference between results from the MSC-EVs and control groups. Animal survival was analyzed employing the Kaplan–Meier log-rank method. Statistical analysis was performed with GraphPad Prism (version 6.07, GraphPad Software). $p < 0.05$ were considered to be statistically significant.

4 | RESULTS

4.1 | Isolation and identification of BM-MSCs and extracellular vesicles derived from mesenchymal stem cells

BM-MSCs were isolated and cultured from C57BL/6 mice. The BM-MSCs were harvested at passage 2 to analyze the immunophenotype with flow cytometry. As shown in Figure 1a, the BM-MSCs expressed CD105, CD73, and CD90, and not CD34, CD45, and HLA-DR. BM-MSCs had a monolayer of bipolar spindle-like cells. BM-MSCs were differentiated into adipocytes and osteoblasts as described in methods (Figure 1b).

4.2 | Extracellular vesicle characterization

Ultrafiltration followed by SEC was used to isolate EVs from the BM-MSC conditioned medium. The average size and morphology of the EVs were evaluated by DLS, field emission scanning electron microscope, and TEM. We evaluated different fractions of isolated EVs by SEC. Fractions 8–10 represented our main group of EVs. The presence of isolated EVs was confirmed by electron microscopy imaging. The size range of the EVs was 95–200 nm, and EVs were round and spherical (Figure 1c,d,f). Western blot analysis confirmed that the MSC-EVs were positive for the general EV-specific markers CD9 and CD63, which both were detectable, albeit weakly, also in their parent cells (Figure 1e). Taken together, characterization of EVs in terms of size, morphology, and specific markers suggested EVs.

4.2.1 | Assessment of extracellular vesicles uptake by splenocytes

We assessed the ability of the splenocytes to taken up EVs. MSC-EVs were labeled with PKH26 dye and incubated for 6 h with splenocytes. Then, the cells were fixed and stained with DAPI. Figure 2a shows the internalization and localization of PKH-26 red-labeled EVs in the cytoplasm of the splenocytes.

4.2.2 | Extracellular vesicles derived from mesenchymal stem cells can inhibit splenocytes proliferation

MSC-EVs have been reported to suppress the proliferation of activated T cells. To investigate whether MSCs-EVs have an inhibitory effect on splenocytes, we evaluated the proliferation of splenocytes in response to increasing doses of MSC-EVs. Figure 2b and c shows the inhibitory effect of MSC-EVs on splenocyte proliferation. Splenocytes were treated with 50 μg Hx-EVs and Nx-EVs for 24 and 48 h, and then assessed the expression levels of the anti-inflammatory miRNAs in splenocytes and the level of inflammatory cytokines (IFN-γ and TNF-α) that were secreted in the conditioned medium. The level of these

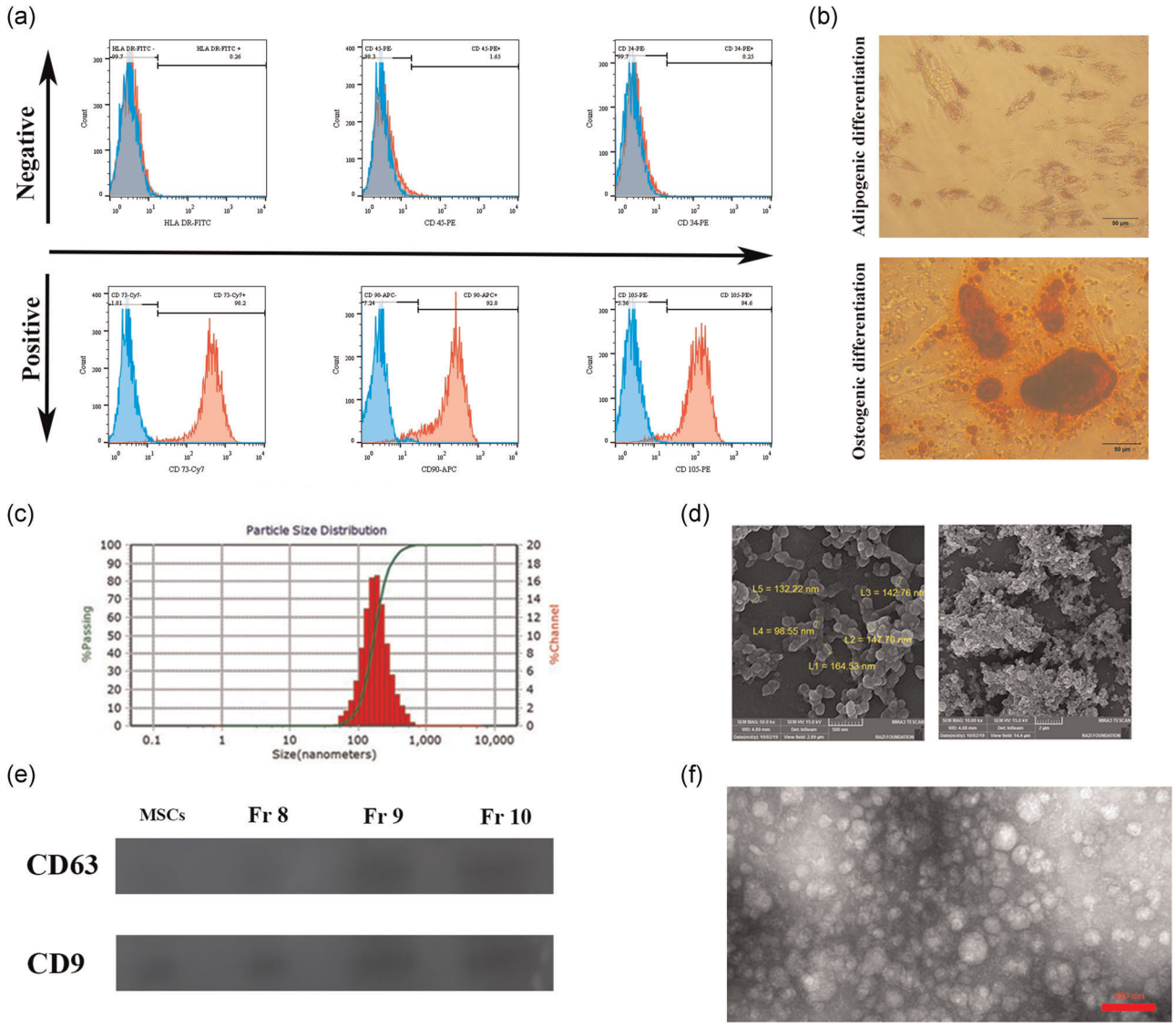

FIGURE 1 Characterization of BM-MSCs and extracellular vesicles derived from mesenchymal stem cells (MSC-EVs). Immunophenotypes of the BM-MSCs were examined by flow cytometry. The vast majority of cells (>90%) were positive for CD73, CD90, and CD105. Few cells expressed CD45, CD34, and Human Leukocyte Antigen – DR (HLA-DR) (a). The BM-MSCs were cultured in osteogenic and adipogenic induction media for 3 weeks, and the induced cells were stained by Alizarin red and oil red O for confirmation of osteocytes and adipocytes, respectively (b). Representative results of dynamic light scattering (DLS) of the MSC-EVs (c). Representative results of the MSC-EVs photographed by a field emission scanning electron microscope and (d and f) transmission electron microscope. Extracellular vesicle (EV) markers of CD9 and CD63 were positive in the three elution fractions collected from size-exclusion chromatographic isolation of MSC-EVs from the conditioned medium was determined by Western blot analysis (e)

cytokines was reduced in the presence of Hx-EVs and Nx-EVs. Notably, at 24 h after treatment, IFN-γ decreased to 204 pg/ml (Nx-EVs) and 178 pg/ml (Hx-EVs) compared to the control group (255 pg/ml; $p < 0.05$). We observed the same scenario with TNF-α. The concentration of TNF-α was 177.78 pg/dl in the control group. Treatment with Nx-EVs (144 pg/dl) and Hx-EVs (48.55 pg/dl) decreased the level of TNF-α ($p < 0.001$) within 24 h. We further examined the effect of MSC-EVs treatment after 48 h. A further reduction of both cytokines was observed in both treatment groups, but this effect was significantly greater in the Hx-EVs compared to the Nx-EVs. We evaluated the expression level of inflammatory-related miRNAs in MSC-EV treated splenocytes. The results showed that miR-199a and miR-126a did not change in the MSC-EV treated groups compared to the control group. However, miR-223 expression increased significantly after treatment with Nx-EV ($p < 0.01$, 6.34-fold) and Hx-EV ($p < 0.001$, 7.21-fold) at 24 h. At 48 h, Nx-EVs (9.07-fold) and Hx-EVs (8.45-fold) upregulated compared to the control group ($p < 0.001$, Figure 2f). In addition, there was a significantly higher miR-146a observed in the Hx-EV group at 24 h ($p < 0.01$, 4.38-fold) and at 48 h ($p < 0.001$, 8.27-fold, Figure 2f).

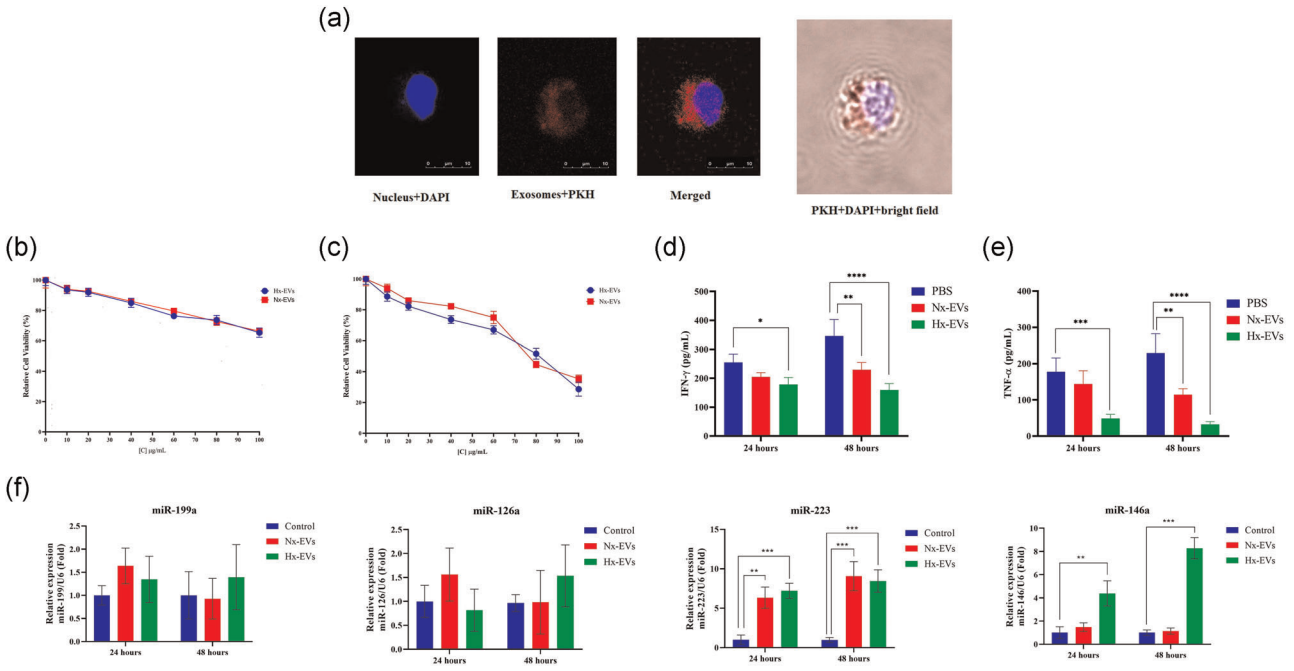

FIGURE 2 Alteration of proliferation, cytokine production, and gene expression in splenocytes treated by extracellular vesicles derived from mesenchymal stem cells (MSC-EVs). Confocal images of T cells after a 6-h incubation with MSC-EVs. DAPI was used to stain the nuclei (blue), and MSC-EVs were labeled with PKH26 (red). Scale bars: 20 μm (a). The proliferation of splenocytes significantly reduced in the presence of normoxic MSC-EVs (Nx-EVs) and hypoxic MSC-EVs (Hx-EVs) within 24 and 48 h (b and c). Enzyme-linked immunosorbent assay analyses showed that the levels of TNF-α and IFN-γ were simultaneously decreased by MSC-EVs in splenocytes from C57BL/6 mice ($n = 5$; d and e). Gene expression of the anti-inflammatory microRNAs (miRNAs) was determined using quantitative real-time PCR. MSC-EVs treatment increased the anti-inflammatory miRNA expressions in the stimulated splenocytes. miR-146a, a verified hypoxamiR, was remarkably increased when splenocytes were treated by Hx-EVs and Nx-EVs at 24 and 48 h. miR-223 increased significantly in both the Nx-EV and Hx-EV groups (f). $^{*}p < 0.05$, $^{**}p < 0.01$, $^{***}p < 0.001$, $^{****}p < 0.0001$

4.2.3 | Extracellular vesicles derived from mesenchymal stem cells can ameliorate the phenotype of aplastic anemia model

We induced AA in mice by total body irradiation (3Gy) followed by an IP injection of splenocytes to evaluate the efficiency of the MSC-EVs. Three days later, the mice received twice-weekly IV infusions of Nx-EVs or Hx-EVs (Figure 3a). MSC-EVs were injected into AA mice as long as they were alive. In addition to distinct phenotypes that included weight loss, mental deviation, and decreased activity, the AA mice had clinical evidence of disease progression. As shown in Figure 3b and c, at 21 days after induction of AA, the BM cells were harvested and cultured for 14 days in murine semi-solid media. A dramatic decline in the number of hematopoietic colonies was observed in the AA groups versus the control group in both Nx-EVs and Hx-EVs groups. The most significant decrease was observed in Burst forming unit-erythrocyte (BFU-E, $p < 0.001$), which indicated a significant decline in mature erythrocyte formation. Colony-forming unit granulocyte-erythrocyte-monocyte-macrophage (CFU-GEMM), colony-forming unit granulocyte-macrophages (CFU-GM), and colony-forming unit granulocytes (CFU-G) also had moderate to severe decreases in the numbers of colonies, which supported the idea that remaining HSCs may be functionally unable to support erythroid differentiation.

Immune destruction of HSCs gives rise to pancytopenia, which causes a high mortality rate in AA mice (Figure 3d). The Kaplan–Meier survival curve showed that treatment with Nx-EVs and Hx-EVs improved short-term survival in the AA mice ($p < 0.0001$). The median survival was 33 days for the Nx-EV group and 36 days for the Hx-EV group. This event indicated a similar effect of these MSC-EVs in the AA mice.

In AA, T lymphocytes destroy marrow stem cells by infiltrating BM and secreting excessive levels of anti-hematopoietic cytokines such as IFN-γ and TNF-α. In our study, the level of these cytokines increased significantly in the AA mouse model; however, treatment with Nx-EVs and Hx-EVs significantly reduced the levels of IFN-γ and TNF-α at Days 7 and 14, but not at Day 21. Both pro-inflammatory cytokines increased dramatically. Figure 3e and f demonstrated significant differences between the PBS and Nx-EVs and Hx-EVs groups.

4.3 | Extracellular vesicles derived from mesenchymal stem cells treatment effectively ameliorated the symptoms of aplastic anemia

We elucidated the potential role of Nx-EVs and Hx-EVs on improving the survival rate and decreasing inflammatory cytokines. For this reason, we aimed to assess whether MSC-EVs could be a pivotal microenvironmental

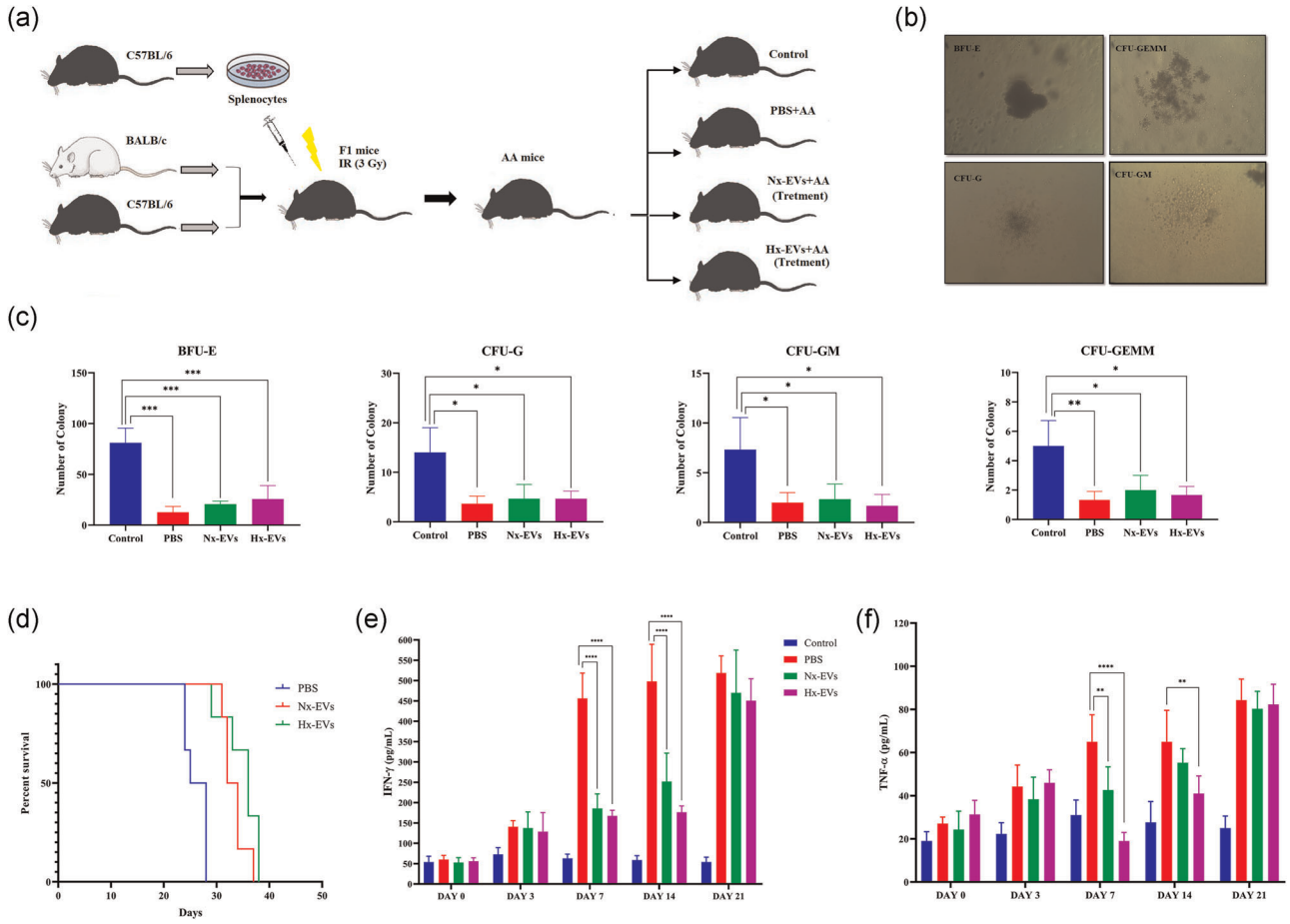

FIGURE 3 Effect of extracellular vesicles derived from mesenchymal stem cells (MSC-EVs) on survival, colony assay, and pro-inflammatory cytokine secretion. The schematic diagram for the development of aplastic anemia (AA) in mice (a). The development of AA reduced the number of hematopoietic colonies in AA bone marrow (BM) as determined by the colony assay (b and c). Survival curves of AA mice treated with normoxic MSC-EVs (Nx-EVs) and hypoxic MSC-EVs (Hx-EVs). Mice that received Nx-EVs and Hx-EVs survived significantly longer than phosphate-buffered saline (PBS) treated mice (d). Pro-inflammatory cytokines interferon-gamma (IFN-γ) and tumor necrosis factor-alpha (TNF-α) were elevated in AA mice. Both downregulated after treatment with both Nx-EVs and Hx-EVs. The significant reduction in these cytokines in our experiment indicated an improvement in the development of AA (e and f). *$p < 0.05$, **$p < 0.01$, ***$p < 0.001$, ****$p < 0.0001$

component for the alleviation of pancytopenia and AA-associated pathological features. We examined BM pathology on Day 14 and compared the cellularity in the BM from each group. Compared with the control group (Figure 4a), the PBS group showed a significant decrease in cellularity, with just a few, sparsely populated islands of residual hematopoiesis. Treatment with Nx-EVs and Hx-EVs clearly positively affected the immune destruction of the HSCs. As shown in Figure 4a, the MSC-EVs treated groups displayed a better hematopoietic activity in the BM. Next, we assessed the BM cell cycle and proliferation in the AA mice. Here, we performed an immunohistochemical assessment of Ki-67 in the BM biopsies. Both the Nx-EVs (12.31 ± 1.30) and Hx-EVs (17.92 ± 3.09) groups had significantly higher Ki67 expression compared with the untreated control (7.28 ± 0.78, Figure 4a,f). These results suggested that the MSC-EVs suppressed the IFN-γ and TNF-α cytokines and had an immunomodulatory effect in immune-mediated AA (Figure 4a,f).

In a similar way, the number of peripheral blood cells, particularly WBCs, showed a remarkable reduction in the AA groups compared with the control group. The WBC counts sharply decreased on Day 3 and this decline continued until Day 21. Treatment with EVs did not improve the status of the WBCs count; therefore, there was no significant difference between untreated and EV treated AA mice. In addition, an insignificant reduction was observed in RBC counts in all untreated and treated AA mice, which could be attributed to the radiation resistance by RBCs. The PLT numbers also declined from Day 7 and this decline continued until Day 21. Although treatment with MSC-EVs did not have a significant effect on WBC and RBC numbers, there was a significant difference between the number of PLT in the PBS and MSC-EVs treated AA mice on Days 7 and 14. Hx-EVs treatment had a more protective effect on the maintenance of PLT numbers.

4.4 | microRNA expression in the in vivo aplastic anemia model

miRNA expression is considered a key mediator in the development of AA, and EVs could be an effective and safe vehicle for therapeutic

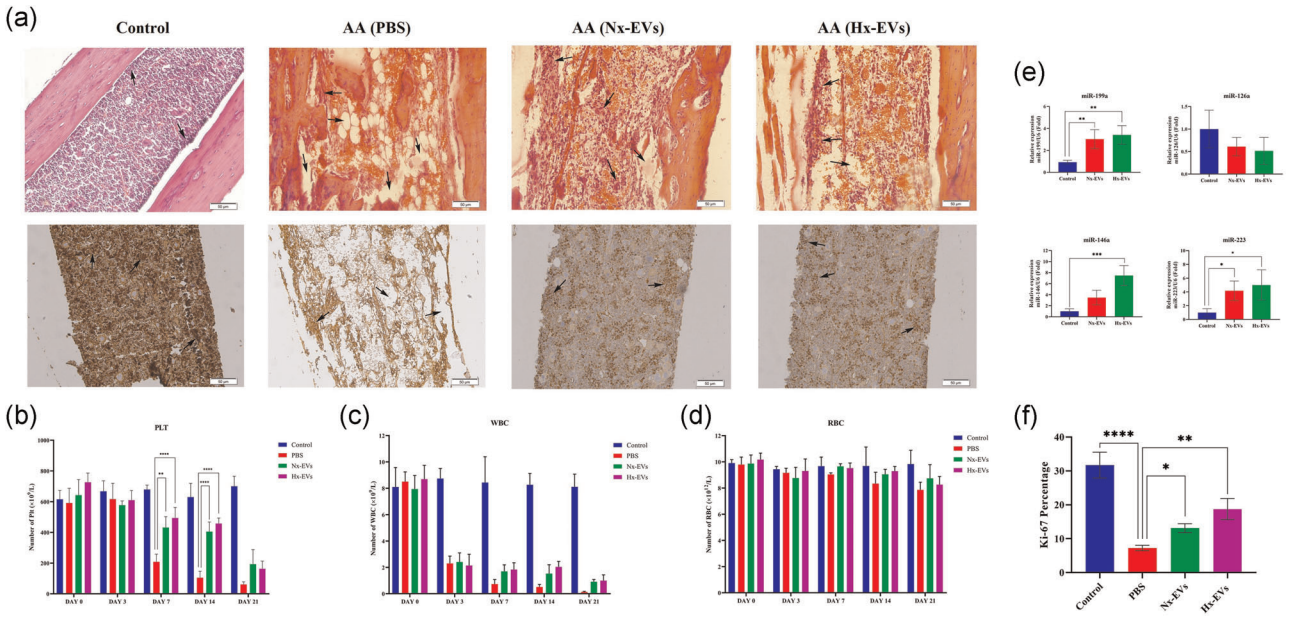

FIGURE 4 Effect of extracellular vesicles derived from mesenchymal stem cells (MSC-EVs) on bone marrow (BM) cellularity and complete blood count (CBC). Histological assessment of BM in aplastic anemia (AA) and control mice. Sections of the BM were stained with hematoxylin-eosin (H&E) and assessed for histological damage 14 days after induction of AA. Ki-67 immunohistological staining was used to observe cell proliferation in bone marrow (BM) on Day 14 after AA induction. This histological observation and statistical analysis represented an obvious hypocellular BM in AA mice, although BM cellularity was markedly better in the normoxic MSC-EVs (Nx-EVs) and hypoxic MSC-EVs (Hx-EVs) treated groups. Representative H&E and immunohistological staining images of the control, phosphate-buffered saline (PBS), Nx-EVs, and Hx-EVs treated groups (a and f). None of the Nx-EVs or Hx-EVs had any effect on red blood cell (RBC) and white blood cell (WBC) counts compared to the PBS group. The RBC counts decreased gradually until Day 21 in all groups. The WBC counts sharply decreased from Day 3; this trend continued until Day 21 (c and d). The platelet (PLT) counts showed a different pattern with a significant decrease after Day 7. The Nx-EVs and Hx-EVs groups showed significantly higher numbers of PLT compared with the PBS group (b). Gene expressions of the anti-inflammatory microRNAs (miRNAs) were determined using quantitative real-time PCR. MSC-EVs treatment showed upregulation of anti-inflammatory miR-146a, miR-223, and miR-199 at 14 days after AA induction (e). $^{*}p < 0.05$, $^{**}p < 0.01$, $^{***}p < 0.001$, $^{****}p < 0.0001$

miRNAs treatment. We assessed the relative expressions of several miRNAs—miR-199a, miR-223, miR-126a, and miR-146a, which play a crucial role in the inflammatory response and regulation of inflammatory cytokine gene expressions. We evaluated the expression levels of these miRNAs in BM cells harvested from untreated and treated AA mice on Day 21. The AA mice treated with Nx-EVs ($p < 0.01$, 3.02-fold) and Hx-EVs ($p < 0.01$, 3.4-fold) had increased miR-199a expression. There was no significant change in miR-126a in the Nx-EVs and Hx-EVs groups. miR-223 expression increased in the Nx-EVs ($p < 0.05$, 4.17-fold) and Hx-EVs ($p < 0.05$, 5-fold) groups. miR-146a expression only increased ($p < 0.001$, 7.47-fold) in the Hx-EVs group; however, no changes were observed in the Nx-EVs group (Figure 4e).

5 | DISCUSSION

Abnormal immunity and damage to hematopoietic stem/progenitor cells (HSPCs) mediated by the immune system are major factors in the pathogenesis of AA. Although remarkable improvements have been achieved in the management of AA following IST, up to 30% of patients relapse (Scheinberg et al., 2014). The BM environment might contribute to the abnormal immune response and impaired hematopoietic support. Therefore, researchers have focused on this microenvironment as a possible treatment for inflammatory diseases (Regmi et al., 2019). MSC-EVs can mediate the therapeutic effects of MSCs and affect the immune response, inflammation, cell proliferation, and metabolism (Xie et al., 2020). The quality and therapeutic function of MSCs-EVs is promoted by factors such as hypoxia preconditioning of BM-MSCs and stimulation with IFN-γ (Ren et al., 2019; Zhang et al., 2020). The results of in vitro studies show that hypoxic preconditioning of MSCs generates distinctive changes in stem cell characteristics and influences the secretion of various cytokines and growth factors. Therefore, their results show that hypoxic preconditioning promotes the MSC-EVs therapeutic potency as a potential treatment for immune-mediated inflammatory diseases (Liu et al., 2020). In this study, we have aimed to elucidate the effects of hypoxic and normoxic derived MSC-EVs on an AA mouse model. Busulfan (BU) and radiation were used in two studies to generate a mouse model of BM failure in an attempt to evaluate the ability of MSC-EVs to reverse BM failure. Although these studies investigated BM failure in a pancytopenia mice model, they did not generate immune-mediated AA mice. Therefore, our mouse model more closely resembles the immune pathology of AA and our results are novel (Wen et al., 2016, 2017).

T cell-mediated immune responses should be monitored to avoid the development of AA and other autoimmune or chronic

inflammatory diseases (Zhao et al., 2019). Since T cells play crucial roles in the AA immune response, we initially evaluated the effects of Nx-EVs and Hx-EVs on splenocytes proliferation and cytokine production at 24 and 48 h. Our findings demonstrated that MSC-EVs profoundly reduced the proliferative capacity of splenocytes in a dose-dependent manner. Nx-EVs and Hx-EVs had a similar suppressive effect on splenocytes. There are conflicting results in the literature regarding the ability of MSC-EVs to suppress proliferation, suppression, and activation of T cells. Blazquez et al. (2014) have reported that EVs from human adipose tissue-derived MSCs can suppress T cell proliferation. Amarnath et al. (2015) stated that a possible mechanism of T cell modulation by MSC-EVs could involve adenosine A2A receptors. Although there are also controversial opinions reporting that when phytohemagglutinin (PHA) induced proliferation of PBMC-derived T cells were incubated with MSCs or MSC-EVs, the results showed that MSCs significantly reduced the numbers of T cells compared to incubation with MSC-EVs. MSC-EVs had little but no significant impact (Conforti et al., 2014). These data implied that variations in the immune regulatory function of MSC-EVs would be contingent upon the context of their use; therefore, MSC-EVs should be meticulously assessed for optimization of their therapeutic potential.

Abnormal $CD4^+$ T cells and secreted cytokines play crucial roles in the destruction of HSCs/HPCs in AA. Th1 and Th17 cells increase in number and become activated during the development of AA. Under specific/pathological circumstances, various immune molecules, such as IFN-γ, TNF-α, and numerous ILs (IL-2, 8, 12, 15, 17, and 27) compose a cytokine network that destroys the HSCs/HPCs (Li et al., 2012). We observed that Nx-EV and Hx-EV modulated the splenocyte immune response and suppressed excessive expression of IFN-γ and TNF-α at defined time points. The Hx-EVs had a more profound effect on the inhibition of IFN-γ and TNF-α. Similar to the in vitro study, the MSC-EVs prevented IFN-γ and TNF-α secretion over a period of time in the AA mouse model. The level of these pro-inflammatory cytokines profoundly increased from Day 7 in the AA mice; however, this inflammatory response did not occur in Nx-EVs and Hx-EVs treated mice from Days 7 to 14. Moreover, these significant improvements were not observed on Day 21, which indicated disease progression in the AA mice. It has been reported that MSC-EVs could delay the inflammatory response. Zheng et al. (2020) reported that BM-MSCs-secreted Exo-miR-192-5p reduced the levels of inflammatory cytokines IL-1β and TNF-α in a collagen-induced arthritis rat model. Laso-Gacia et al. noted that MSC-EVs significantly decreased the amounts of IFN-γ (from Th1 cells) and IL-17A (from Th-17 cells). Besides, MSC-EVs also decreased the numbers of inflammatory $CD4^+$ cells in the brain (Laso-García et al., 2018). Hence, we presumed that MSC-EVs could reduce the inflammatory response in mice models of autoimmune diseases. In our study, the short-term effects of MSC-EVs might be due to systematic inflammation in the AA mice.

In the present study, we evaluated HSC/HPC potential within the whole BM-MNC fraction in AA mice. BM-MNCs, including HSCs, were harvested on Day 21 and cultured in methylcellulose semi-solid media to assess their ability to generate hematopoietic colonies. Significantly lower numbers of BFU-E, CFU-GM, CFU-G, and CFU-GEMM colonies were observed in the untreated and MSC-EVs treated AA mice on Day 21. This finding supported the observation of CBCs on Day 21. Over the 21 days, we observed pancytopenia with decreased WBC, RBC, and PLT counts after γ-irradiation and injection of splenocytes. However, there was a gradual decrease in RBC counts with no statistically significant difference noted between RBC counts in the healthy control and AA mice. To some extent, the differences in the colony-forming assay and CBC counts were attributed to the prolonged half-life of nonnucleated RBCs and their resistance to radiation damage. Because of the occurrence of pancytopenia and death within 3–4 weeks in AA mice, we were unable to follow the mice for more than one month and we could not demonstrate that a serious decrease in RBC counts would occur after two months. Our results indicated that the WBC count was not significantly higher in MSC-EVs treated AA mice. Treatment with MSC-EVs did not improve the WBC counts in the AA mice, which could be because of the high sensitivity of WBC, in particular lymphocytes, to radiation and donor T cell attack on marrow cells. We assumed that the immune-mediated AA mice model was a severe type of AA that profoundly activated T cells and attacked BM cells to give rise to BM failure. We assumed that the protective effect of MSC-EVs from radiation damage and suppression of T cells could occur at later time points because the results of previous studies have shown that MSC-EVs significantly ameliorated WBCs at later time points. Accordingly, the MSC-EVs did not effectively ameliorate the number of WBCs. Also, The PLT count began to decline from Day 7. Interestingly, the platelet count remained the same on Days 7 and 14 in the groups treated with Nx-Evs and Hx-EVs, but this protection did not occur on Day 21. We presumed that MSC-EVs temporarily ameliorated AA. Alloreactive T cells gradually attacked the BM cells and caused a severe type of AA, and the immune-modulatory potency of MSC-EVs decreased. Previous studies confirmed that a gross reduction in colonies and clusters in incidence and absolute number in the BM of AA (Barrett et al., 1979; Chatterjee et al., 2010).

Ki-67 is a marker of cell proliferation that is highly expressed during cell replication in G_1, S, G_2, and mitosis, and is absent in resting cells (G_0; Thiele & Fischer, 1993). The expression level of Ki-67 was higher in the BM of MSC-EVs treated AA mice. Lee et al. (1998) reported a very low number of Ki-67 positive cells in the BM of AA patients, which indicated very low proliferative activity. The histological examination in our study also indicated the destruction of BM in the AA mice. The BM cellularity was noticeably higher in MSC-EVs treated AA mice on Day 14, which corresponded with the other results. Similarly, recent studies showed that the conditioned medium or EVs derived from MSCs had an effective therapeutic impact on the reversal of tissue injury. Wen and Quesenberry reported that an IV infusion of MSC-EVs dramatically reversed the radiation damage to BM-HSCs both in vitro and in vivo. Moreover, radiation injury decreased the numbers of WBC and HSCs; however, treatment with MSC-EVs increased WBC and colony formation on irradiated BM cells (Wen et al., 2016). In another study related to BM

failure, BU induced AA mice were infused with human MSC-EVs from days one to three after the final BU dose. The human MSC-EVs treatment significantly prolonged survival and augmented the BM cell count (Wen et al., 2017). Our findings supported those of other investigators where MSC-EVs had the potential to delay AA. The BU induced model is beneficial for assessing myelotoxic agents and it shows the tremendous compensatory capacity of BM, which permits limited numbers of HSCs to produce normal levels of blood cells; however, it did not address the likely immune mechanism of most acquired AA and the disease was unaffected by cyclosporine treatment (Chen et al., 2004).

In this study, we also sought to determine if MSC-EVs could affect the immune responses via miRNAs. Thus, the expression levels of selected miRNAs including miR-146a, miR-126a, miR199a, and miR-223 were evaluated in MSC-EV treated splenocytes AA mouse. These miRNAs carried by MSC-EVs and play a crucial role in cellular immune modulation (Giudice et al., 2018; Hosokawa et al., 2014). In addition, high levels of these miRNAs were reported in MSC-EVs, particularly those stimulated by hypoxia. We used hypoxia rather than genetic modification or transfection to induce the expression level of our candidate miRNAs. Previous studies confirmed that hypoxic conditions could augment the immunoregulatory effects of EVs and this potential ability was carried via miRNAs (Lo Sicco et al., 2017; Nallamshetty et al., 2013). The results of in vitro and in vivo studies demonstrated that miR-223 expression profoundly increased in Nx-EVs and Hx-EVs treated splenocytes and AA mice. It has been reported that miR-223, miR-199a, and miR-126 were downregulated in T cell populations of AA patients. Moreover, those patients had an effective IST and the expression levels of these miRNAs increased to normal levels (Hosokawa et al., 2014). Several studies investigated the use of miR-223 that contained exosomes as a valuable tool for improving inflammatory disorders. Chen et al. have reported that miR-223 is highly expressed in BM-MSCs and plays an important role in autoimmune diseases. BM-MSCs-exo$^{miR\text{-}223(+)}$ significantly downregulated the expressions of inflammatory cytokines TNF-α and IL-1β, and improved autoimmune hepatitis in mice (Chen et al., 2018). Another study also indicated the potential role of microvesicle-containing miR-223 in a mice model of lung inflammation. They found that the miR-223/142-enriched microvesicles selectively targeted lung macrophages and suppressed the inflammatory lung responses (Zhang et al., 2019). High levels of miR-146a were verified in mammalian cells under hypoxic conditions (Nallamshetty et al., 2013). Similarly, we observed that the level of miR-146a was only enhanced in the Hx-EV treated group. The enhanced therapeutic efficacy of IL-1β-primed MSCs against sepsis was shown by exosome-containing miR-146a (Song et al., 2017). In addition, the effect of EVs that contained miR-146a was studied in colitis. These EVs ameliorated experimental colitis by targeting TRAF6 and IRAK1 (Wu et al., 2019). Similarly, we observed that increased BM expressions of miR-223a and miR-146a significantly alleviated the pathological manifestations of acute inflammatory disorders in the AA mouse model.

In conclusion, our findings add substantially to our understanding of the therapeutic effect of MSC-EVs. It seems reasonable to presume that MSC-EVs temporally ameliorate BM failure and attenuate AA progression by modulating immune reactivity. Our study results have shown that hypoxic and normoxic MSC derived EVs suppressed T cell proliferation, regulated the expression of inflammatory cytokines, and prolonged the survival rate in a mouse model of AA. Therefore, MSC-EVs should be considered as a potential therapeutic approach for the treatment of AA.

ACKNOWLEDGMENTS

This study was supported by Tarbiat Modares University, Council for Development of Stem Cell Sciences and Technologies, and Iran National Science Foundation.

CONFLICT OF INTERESTS

The authors declare that there are no conflict of interests.

ETHICS STATEMENT

All applicable international, national, and/or institutional guidelines for the care and use of animals were followed.

AUTHOR CONTRIBUTIONS

Saeid Abroun and Mohammad A. Gholampour conceived and designed the experiments. Mohammad A. Gholampour performed the experiments; Sara Soudi and Seyed J. Mowla drafted the manuscript. Rienk Nieuwland and Saeid Abroun prepared and reviewed the manuscript. Saeid Abroun and Rienk Nieuwland have given final approval of the version to be published. All authors have read and approved the manuscript.

DATA AVAILABILITY STATEMENT

The data that support the findings of this study are available from the corresponding author on reasonable request.

ORCID

Saeid Abroun https://orcid.org/0000-0003-3853-1256
Sara Soudi http://orcid.org/0000-0002-8978-3958

REFERENCES

Amarnath, S., Foley, J. E., Farthing, D. E., Gress, R. E., Laurence, A., Eckhaus, M. A., Métais, J. Y., Rose, J. J., Hakim, F. T., Felizardo, T. C., Cheng, A. V., Robey, P. G., Stroncek, D. E., Sabatino, M., Battiwalla, M., Ito, S., Fowler, D. H., & Barrett, A. J. (2015). Bone marrow-derived mesenchymal stromal cells harness purinergenic signaling to tolerize human T h1 cells in vivo. *Stem Cells*, *33*(4), 1200–1212.

Barrett, A., Faille, A., Balitrand, N., Ketels, F., & Najean, Y. (1979). Bone marrow culture in aplastic anemia. *Journal of Clinical Pathology*, *32*(7), 660–665.

Blazquez, R., Sanchez-Margallo, F. M., de la Rosa, O., Dalemans, W., Álvarez, V., Tarazona, R., & Casado, J. G. (2014). Immunomodulatory potential of human adipose mesenchymal stem cells derived exosomes on in vitro stimulated T cells. *Frontiers in Immunology*, *5*, 556.

Boddu, P. C., & Kadia, T. M. (2019). Molecular pathogenesis of acquired aplastic anemia. *European Journal of Haematology*, *102*(2), 103–110.

Brzeźniakiewicz-Janus, K., Rupa-Matysek, J., & Gil, L. (2020). Acquired aplastic anemia as a clonal disorder of hematopoietic stem cells. *Stem Cell Reviews and Reports*, *16*, 1–10.

Böing, A. N., Van Der Pol, E., Grootemaat, A. E., Coumans, F. A., Sturk, A., & Nieuwland, R. (2014). Single-step isolation of extracellular vesicles by size-exclusion chromatography. *The Journal of Extracellular Vesicles*, *3*.

Canzano, F., Paganelli, A., Volpe, P., & Paganelli, R. (2018). The role of miRNAs in autoimmune inflammatory diseases. *International Journal of Clinical Rheumatology*, *13*(6), 360.

Chatterjee, S., Dutta, R. K., Basak, P., Das, P., Das, M., Pereira, J. A., Chaklader, M., Chaudhuri, S., & Law, S. (2010). Alteration in marrow stromal microenvironment and apoptosis mechanisms involved in aplastic anemia: An animal model to study the possible disease pathology. *Stem Cells International*, *2010*, 1–12.

Chen, J., Lipovsky, K., Ellison, F. M., Calado, R. T., & Young, N. S. (2004). Bystander destruction of hematopoietic progenitor and stem cells in a mouse model of infusion-induced bone marrow failure. *Blood*, *104*(6), 1671–1678.

Chen, L., Lu, F., Chen, D., Wu, J., Hu, E., Xu, L., Zheng, M., Li, H., Huang, Y., Jin, X., Gong, Y., Lin, Z., Wang, X., & Chen, Y. (2018). BMSCs-derived miR-223-containing exosomes contribute to liver protection in experimental autoimmune hepatitis. *Molecular Immunology*, *93*, 38–46.

Conforti, A., Scarsella, M., Starc, N., Giorda, E., Biagini, S., Proia, A., Locatelli, F., & Bernardo, M. E. (2014). Microvesicles derived from mesenchymal stromal cells are not as effective as their cellular counterpart in the ability to modulate immune responses in vitro. *Stem Cells and Development*, *23*(21), 2591–2599.

Duan, P., Tan, J., Miao, Y., & Zhang, Q. (2019). Potential role of exosomes in the pathophysiology, diagnosis, and treatment of hypoxic diseases. *American Journal of Translational Research*, *11*(3), 1184.

Eleuteri, S., & Fierabracci, A. (2019). Insights into the secretome of mesenchymal stem cells and its potential applications. *International Journal of Molecular Sciences*, *20*(18), 4597.

Fan, X.-L., Zhang, Y., Li, X., & Fu, Q.-L. (2020). Mechanisms underlying the protective effects of mesenchymal stem cell-based therapy. *Cellular and Molecular Life Sciences*, *77*, 1–24.

Giudice, V., Banaszak, L. G., Gutierrez-Rodrigues, F., Kajigaya, S., Panjwani, R., Ibanez, M. P. F., Rios, O., Bleck, C. K., Stempinski, E. S., Raffo, D. Q., Townsley, D. M., & Young, N. S. (2018). Circulating exosomal microRNAs in acquired aplastic anemia and myelodysplastic syndromes. *Haematologica*, *103*(7), 1150–1159.

Hosokawa, K., Kajigaya, S., Feng, X., Desierto, M. J., Fernandez Ibanez, M. P., Rios, O., Weinstein, B., Scheinberg, P., Townsley, D. M., & Young, N. S. (2017). A plasma microRNA signature as a biomarker for acquired aplastic anemia. *Haematologica*, *102*(1), 69–78.

Hosokawa, K., Muranski, P., Feng, X., Keyvanfar, K., Townsley, D. M., Dumitriu, B., & Hourigan, C. S. (2014). *Altered microRNAs in T cells from patients with acquired aplastic anemia*. American Society of Hematology.

Kornilov, R., Puhka, M., Mannerström, B., Hiidenmaa, H., Peltoniemi, H., Siljander, P., Seppänen-Kaijansinkko, R., & Kaur, S. (2018). Efficient ultrafiltration-based protocol to deplete extracellular vesicles from fetal bovine serum. *Journal of Extracellular Vesicles*, *7*(1), 1422674.

Laso-García, F., Ramos-Cejudo, J., Carrillo-Salinas, F. J., Otero-Ortega, L., Feliú, A., Gómez-de Frutos, M., Mecha, M., Díez-Tejedor, E., Guaza, C., & Gutiérrez-Fernández, M. (2018). Therapeutic potential of extracellular vesicles derived from human mesenchymal stem cells in a model of progressive multiple sclerosis. *PLOS One*, *13*(9): e0202590.

Lee, J. N., Park, J. I., & Kim, M. Y. (1998). Expression of Ki-67/MIB-1 in bone marrow biopsies from patients with myelodysplastic syndromes and aplastic anemia. *Korean Journal of Clinical Pathology*, *18*(4), 511–515.

Li, J., Lu, S., Yang, S., Xing, W., Feng, J., Li, W., Zhao, Q., Wu, H., Ge, M., Ma, F., Zhao, H., Liu, B., Zhang, L., Zheng, Y., & Han, Z. C. (2012). Impaired immunomodulatory ability of bone marrow mesenchymal stem cells on CD4+ T cells in aplastic anemia. *Results in Immunology*, *2*, 142–147.

Liu, W., Li, L., Rong, Y., Qian, D., Chen, J., Zhou, Z., Luo, Y., Jiang, D., Cheng, L., Zhao, S., Kong, F., Wang, J., Zhou, Z., Xu, T., Gong, F., Huang, Y., Gu, C., Zhao, X., Bai, J., … Cai, W. (2020). Hypoxic mesenchymal stem cell-derived exosomes promote bone fracture healing by the transfer of miR-126. *Acta Biomaterialia*, *103*, 196–212.

Nallamshetty, S., Chan, S. Y., & Loscalzo, J. (2013). Hypoxia: A master regulator of microRNA biogenesis and activity. *Free Radical Biology and Medicine*, *64*, 20–30.

Phelps, J., Sanati-Nezhad, A., Ungrin, M., Duncan, N. A., & Sen, A. (2018). Bioprocessing of mesenchymal stem cells and their derivatives: Toward cell-free therapeutics. *Stem Cells International*, *2018*, 1–23.

Regmi, S., Pathak, S., Kim, J. O., Yong, C. S., & Jeong, J.-H. (2019). Mesenchymal stem cell therapy for the treatment of inflammatory diseases: Challenges, opportunities, and future perspectives. *European Journal of Cell Biology*, *98*(5–8), 151041.

Ren, L., Song, Z., Cai, Q., Chen, R., Zou, Y., Fu, Q., & Ma, Y.-Y. (2019). Adipose mesenchymal stem cell-derived exosomes ameliorate hypoxia/serum deprivation-induced osteocyte apoptosis and osteocyte-mediated osteoclastogenesis in vitro. *Biochemical and Biophysical Research Communications*, *508*(1), 138–144.

Roderick, J. E., Gonzalez-Perez, G., Kuksin, C. A., Dongre, A., Roberts, E. R., Srinivasan, J., Andrzejewski, C., Fauq, A. H., Golde, T. E., Miele, L., & Minter, L. M. (2013). Therapeutic targeting of NOTCH signaling ameliorates immune-mediated bone marrow failure of aplastic anemiaNOTCH1 signaling in BM failure. *The Journal of Experimental Medicine*, *210*(7), 1311–1329.

Scheinberg, P., Rios, O., Scheinberg, P., Weinstein, B., Wu, C. O., & Young, N. S. (2014). Prolonged cyclosporine administration after antithymocyte globulin delays but does not prevent relapse in severe aplastic anemia. *American Journal of Hematology*, *89*(6), 571–574.

Seo, Y., Kim, H.-S., & Hong, I.-S. (2019). Stem cell-derived extracellular vesicles as immunomodulatory therapeutics. *Stem Cells International*, *2019*, 1–10.

Lo Sicco, C., Reverberi, D., Balbi, C., Ulivi, V., Principi, E., Pascucci, L., Becherini, P., Bosco, M. C., Varesio, L., Franzin, C., Pozzobon, M., Cancedda, R., & Tasso, R. (2017). Mesenchymal stem cell-derived extracellular vesicles as mediators of anti-inflammatory effects: Endorsement of macrophage polarization. *Stem Cells Translational Medicine*, *6*(3), 1018–1028.

Song, Y., Dou, H., Li, X., Zhao, X., Li, Y., Liu, D., Ji, J., Liu, F., Ding, L., Ni, Y., & Hou, Y. (2017). Exosomal miR-146a contributes to the enhanced therapeutic efficacy of interleukin-1β-primed mesenchymal stem cells against sepsis. *Stem Cells*, *35*(5), 1208–1221.

Thiele, J., & Fischer, R. (1993). *Bone marrow tissue and proliferation markers: Results and general problems*. Springer.

Trubiani, O., Marconi, G. D., Pierdomenico, S. D., Piattelli, A., Diomede, F., & Pizzicannella, J. (2019). Human oral stem cells, biomaterials and extracellular vesicles: A promising tool in bone tissue repair. *International Journal of Molecular Sciences*, *20*(20), 4987.

Wang, X., Gu, H., Qin, D., Yang, L., Huang, W., Essandoh, K., Wang, Y., Caldwell, C. C., Peng, T., Zingarelli, B., & Fan, G. C. (2015). Exosomal miR-223 contributes to mesenchymal stem cell-elicited cardioprotection in polymicrobial sepsis. *Scientific Reports*, *5*, 13721.

Weiss, A. R. R., & Dahlke, M. H. (2019). Immunomodulation by mesenchymal stem cells (MSCs): Mechanisms of action of living, apoptotic, and dead MSCs. *Frontiers in Immunology*, *10*, 1191.

Wen, S., Dooner, M., Cheng, Y., Papa, E., Del Tatto, M., Pereira, M., Deng, Y., Goldberg, L., Aliotta, J., Chatterjee, D., Stewart, C., Carpanetto, A., Collino, F., Bruno, S., Camussi, G., & Quesenberry, P. (2016). Mesenchymal stromal cell-derived extracellular vesicles

rescue radiation damage to murine marrow hematopoietic cells. *Leukemia*, *30*(11), 2221–2231.

Wen, S., Dooner, M. S., Papa, E., Del Tatto, M., Pereira, M., Cheng, Y., & Quesenberry, P. (2017). Reversal of aplastic anemia by mesenchymal stem cell-derived extracellular vesicles. *Blood*, *130*(Suppl 1), S2456.

Wu, H., Fan, H., Shou, Z., Xu, M., Chen, Q., Ai, C., Dong, Y., Liu, Y., Nan, Z., Wang, Y., Yu, T., & Liu, X. (2019). Extracellular vesicles containing miR-146a attenuate experimental colitis by targeting TRAF6 and IRAK1. *International Immunopharmacology*, *68*, 204–212.

Xie, M., Xiong, W., She, Z., Wen, Z., Abdirahman, A. S., Wan, W., & Wen, C. (2020). Immunoregulatory effects of stem cell-derived extracellular vesicles on immune cells. *Frontiers in Immunology*, *11*.

Zhang, X. (2016). Endothelial HSPA12B is a novel protein for the preservation of cardiovascular function in polymicrobial sepsis via exosome miR-126. *Frontiers in Immunology*.

Zhang, D., Lee, H., Wang, X., Groot, M., Sharma, L., Cruz, C. S. D., & Jin, Y. J. T. (2019). A potential role of microvesicle-containing miR-223/142 in lung inflammation. *Thorax*, *74*(9), 865–874.

Zhang, G., Zhu, Z., Wang, H., Yu, Y., Chen, W., Waqas, A., Wang, Y., & Chen, L. (2020). Exosomes derived from human neural stem cells stimulated by interferon gamma improve therapeutic ability in ischemic stroke model. *Journal of Advanced Research*, *24*, 435–445.

Zhao, J., Chen, J., Huang, F., Wang, J., Su, W., Zhou, J., & Liu, Z. (2019). Human gingiva tissue-derived MSC ameliorates immune-mediated bone marrow failure of aplastic anemia via suppression of Th1 and Th17 cells and enhancement of CD4+ Foxp3+ regulatory T cells differentiation. *American Journal of Translational Research*, *11*(12), 7627.

Zheng, J., Zhu, L., In, I. I., Chen, Y., Jia, N., & Zhu, W. (2020). Bone marrow-derived mesenchymal stem cells-secreted exosomal microRNA-192-5p delays inflammatory response in rheumatoid arthritis. *International Immunopharmacology*, *78*, 105985.

SUPPORTING INFORMATION

Additional supporting information may be found online in the Supporting Information section.

How to cite this article: Gholampour MA, Abroun S, Nieuwland R, Mowla SJ, Soudi S. Mesenchymal stem cell-derived extracellular vesicles conditionally ameliorate bone marrow failure symptoms in an immune-mediated aplastic anemia mouse model. *J Cell Physiol*. 2021;236:6055–6067. https://doi.org/10.1002/jcp.30291